*Materials Science Forum Vols. 492-493 (2005) pp. 621-626*
*online at http://www.scientific.net*


# Evaluation of SiC-particle Connectivity in Functionally Graded Al/SiC$_p$ Composites by Synchrotron Radiation Holographic Microtomography

A. Velhinho[1,2,a], G. L. Vignoles[3,b], P. Cloetens[4,c], X. Thibault[4,d], E. Boller[4,e], F. Braz Fernandes[1,2,f], L.A. Rocha[5,6,g] and J.D. Botas[1,h]

[1]CENIMAT – Centro de Investigação em Materiais, Univ. Nova de Lisboa – Portugal

[2]DCM –Dep. Ciência dos Materiais, Fac. Ciências e Tecnologia, Univ. Nova de Lisboa – Portugal

[3]LCTS – Laboratoire des Composites Thermostructuraux, Univ. de Bordeaux 1 – France

[4]ESRF – European Synchrotron Radiation Facility – France

[5]CIICS – Centro de Investigação de Interfaces e Comportamento de Superfícies, Univ. do Minho – Portugal

[6]DEM – Dep. Engenharia Mecânica, Escola de Engenharia, Univ. do Minho – Portugal

[a]ajv@fct.unl.pt, [b]vinhola@lcts.u-bordeaux1.fr, [c]cloetens@esrf.fr, [d]boller@esrf.fr, [e]thibault@esrf.fr, [f]fbf@fct.unl.pt, [g]lrocha@dem.uminho.pt, [h]jdb@fct.unl.pt

**Keywords:** Particle connectivity. MMC. FGMMC. Microtomography. Holotomography. Synchrotron radiation.

**Abstract.** Reliability of functionally graded metal matrix composites (FGMMCs) for automotive components is still dependent on the detailed knowledge of the mechanisms of the microstructural build-up, for instance on the mechanisms leading to the distribution and relative positions of the reinforcing particles. In order to assess the influence of the SiC particle size on the 3-D inter-particle connectivity in functionally graded Al/SiCp composites produced by centrifugal casting, X-ray microtomography experiments were performed at the ID19 beamline in ESRF (European Synchrotron Radiation Facility). The FGMMCs consisted of an Al-10Si-2Mg alloy matrix, reinforced by an average SiC particle volume fraction of 0.10; two different average sizes were used: 37 μm and 12 μm. The holographic modification of the X-ray CMT (Computer Micro-Tomography) method allowed to obtain neatly contrasted images, as opposed to classical CMT.Good agreement was found between the particle size evaluated by CMT and by laser interferometry. Particle clustering has been evaluated in number and volume, showing that a lower mean particle size is related to more clustering. Such an adverse effect relies on the importance of particle/liquid alloy surface tension. Also, the mean particle size has been evaluated as a function of particle number within a cluster: as expected, the larger a cluster, the larger the particles inside it.

## Introduction

The concept of functionally graded material (FGM) is particularly interesting to be applied in components for the automotive industry, if reliability and cost can be controlled in an advantageous way. Centrifugal casting of SiC reinforced Al-alloys is, from the economical point of view, a promising technique to be used in the fabrication of such components. However, reliability is still dependent on the detailed knowledge of the mechanisms leading to the distribution and relative positions of the reinforcing particles [1].

FGMMCs feature engineered gradual transitions in volume fraction of reinforcement and/or particle size, in order to be used in components combining localized high wear resistance with high bulk toughness. For any Al/SiC$_p$ composite, the reinforcement distribution has a two-fold relevance. First, the presence of reinforcing particles is directly implied on the local mechanical properties, with reflection on the overall properties of the composite [2]. On the other hand, the presence of reinforcement clusters will bring a higher probability of crack nucleation, i.e. fatigue failure [2].

Furthermore, for FGMMCs the existence of both reinforcement-rich and reinforcement-poor regions is inherent to the very nature of the material. In such a case, a smooth transition between those regions must be assured, while at the same time avoiding particle clustering or total depletion. This can only be achieved through a fine balance between the velocity imparted to the particles and the advance of the solidification front [3, 4].

The present work comes as a complement of previous studies where 2-D characterization techniques already gave some insight to the particle distribution [3-5], but could not, by its nature, provide 3-D stereological information, namely inter-particle connectivity [6]. Previous X-ray micro-tomography experiments carried out at the ID19 beamline in ESRF were useful to assess the interaction among SiC particles, the aluminium matrix, and voids formed due to incomplete wetting of the two constituents [7, 8]. Partly as a result of those experiments, the matrix composition was changed from Al – 7 Si – 0.4 Mg to Al – 10 Si – 2 Mg; improved wetting characteristics were obtained through an increase in Mg content [9], aiming at minimizing void formation. However, those ESRF experiments were performed using the absorption contrast acquisition mode; given the similar absorption coefficients of Al and SiC, this led to segmentation difficulties. Such problems were overcome in the present work through the use of the holotomography technique, which provides density maps and therefore a clear contrast between the different phases [10].

## Experimental

Single precursor conventional MMCs were prepared by rheocasting from an Al – 10 Si – 2 Mg alloy and SiC particles; the mean particle sizes, as measured with a Coulter LS230 laser interpherometer, being $D_V = 12$ μm and $D_V = 37$ μm. Overall particle volume fraction in every case was $f_R = 0.10$. Subsequently, the MMCs were molten and centrifugally cast using a Linn High Therm Titancast 700 μP Vac furnace, in order to obtain two functionally graded composites, each one reinforced by particles of different size. Details of both processes are available elsewhere [3, 4, 6, 11].

From each FGMMC, cylindrical samples, around 1 mm in diameter and 30 mm long, were machined by EDM. The axis of each sample was parallel to the (longitudinal) direction of the functional gradient. The original positions of the samples defined a regular grid.

The samples were analysed by X-ray microtomography at the ID 19 beamline of the European Synchrotron Radiation Facility, in Grenoble. Selected Regions of Interest (ROI) were scanned along each sample. For the purposes of the present work, ROI positioning is schematised in Fig. 1, whereas the approximate centre coordinates are presented in Table 1.

Table 1: ROI coordinates, according the spatial orientation presented in Fig. 1.

| **ROI** | A1 | A2 | A3 | A4 | B5 |
|---|---|---|---|---|---|
| **FGMMC** | A | | | | B |
| **Particle size [μm]** | 37 | | | | 12 |
| **X** | -5 | 0 | -5 | -15 | -5 |
| **Y** | 0 | 5 | 0 | | |
| **Z** | 2 | | 7 | 2 | |

The microtomographic measurements were performed with a beam energy of 20 keV, and a multilayer was used as monochromator. For each sample, several sample ↔ detector distances were used (100, 200 and 400 mm). The detector consisted of a FRELON 1024*1024 CCD camera. Through superposition of the images obtained with different distances, holotomographic images were obtained, in order to enhance contrast between SiC particles and aluminium matrix. *Voxel* size was $1.20^3$ μm$^3$.

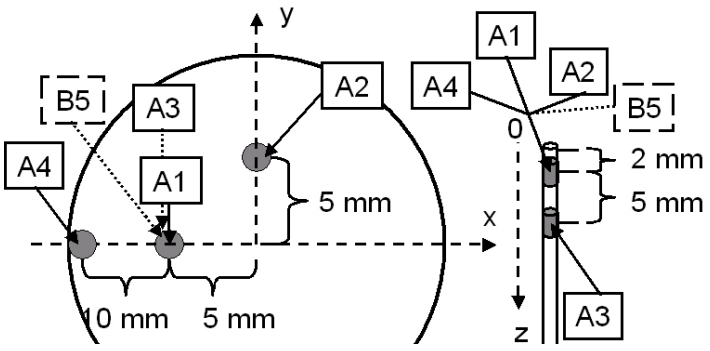


Fig. 1: ROI schematic positioning. Two samples, each located at 5 mm from the centre, and placed over two orthogonal axis ($\overline{Ox}$ and $\overline{Oy}$) of the FGM, were considered for this work. ROI positioning along the samples corresponded to vertical positions (along the $\overline{Oz}$ longitudinal functional gradient axis of the material) of 2 and 7 mm.

Image segmentation and 3-D particle analysis were performed at LCTS. Segmentation has been straightforward, since the contrast provided by the holotomographic method was excellent. The particles were identified by a classical image invasion algorithm, with a simultaneous identification of their surface and volume. They have been partially separated by a one-voxel-depth erosion and a new invasion of the eroded particles. The number of connected subsets has been recorded for every particle, thus allowing (i) to perform statistical analysis on cluster number and volume, and (ii) to improve the analysis of particle data. In order to avoid edge effects, this treatment was applied to sub-sets of each ROI, henceforward designated as Volume of Interest (VOI). The average dimension of VOIs A1 to A4 was $655 \times 660 \times 900$ *voxels* (0,67 $mm^3$); however, due to calculation time limitations (calculation time is more strongly dependent on the number of reconstructed objects to separate than on VOI volume), VOI B5 had to be restricted to $710 \times 710 \times 135$ *voxels* (0,12 $mm^3$). As the number of contacting particles within a cluster increases, there are less and less clusters of that type in the image, so this renders the data for large clusters less reliable; however, the relative volume and number of isolated particles and small clusters have been assessed with a reasonable level of uncertainty. Indeed, VOIs A1 to A4 contained approximately 3000 particles, and VOI B5 2000 particles. The particle size estimation has been made with the approximation of sphericity (*i.e.* $D_V = [6\ V / \pi]^{1/3}$); the aspect ratio ($S^3 / V^2$) has been checked to be close to the spherical value.

## Results and Discussion

In Fig. 2, the particle size distributions regarding the reconstructed tomographic objects are compared to those corresponding to the raw SiC particles, as measured before MMC fabrication. A good agreement is found between the size of the reconstructed particles and that of the raw particles, for those cases corresponding to 35 μm; for the smaller 12 μm particles the agreement reached is still satisfactory, even if the tomographic objects seem slightly undersized, and if the filtering applied in order to reduce noise is responsible for the deletion of the low-end distribution tail. However, one should bear in mind that the raw particle distribution is not entirely representative of the particle sizes found in the FGMMC, due to a dimensional segregation effect induced by centrifugal casting [3-5, 11].

The values determined through X-ray microtomography for the particle volume fraction – $f_R$ – are presented in Table 2. It can be seen that ROI A3, corresponding to a larger distance from the surface than the other ROIs in FGMMC A, exhibits a slightly higher $f_R$ value, which again is consistent with earlier observations [3-5, 11].

Table 2: Particle volume fraction determined by microtomography.

| ROI | A1 | A2 | A3 | A4 | B5 |
|---|---|---|---|---|---|
| $f_R$ | $8.80 \times 10^{-2}$ | $9.79 \times 10^{-2}$ | $10.02 \times 10^{-2}$ | $9.60 \times 10^{-2}$ | $10.89 \times 10^{-2}$ |

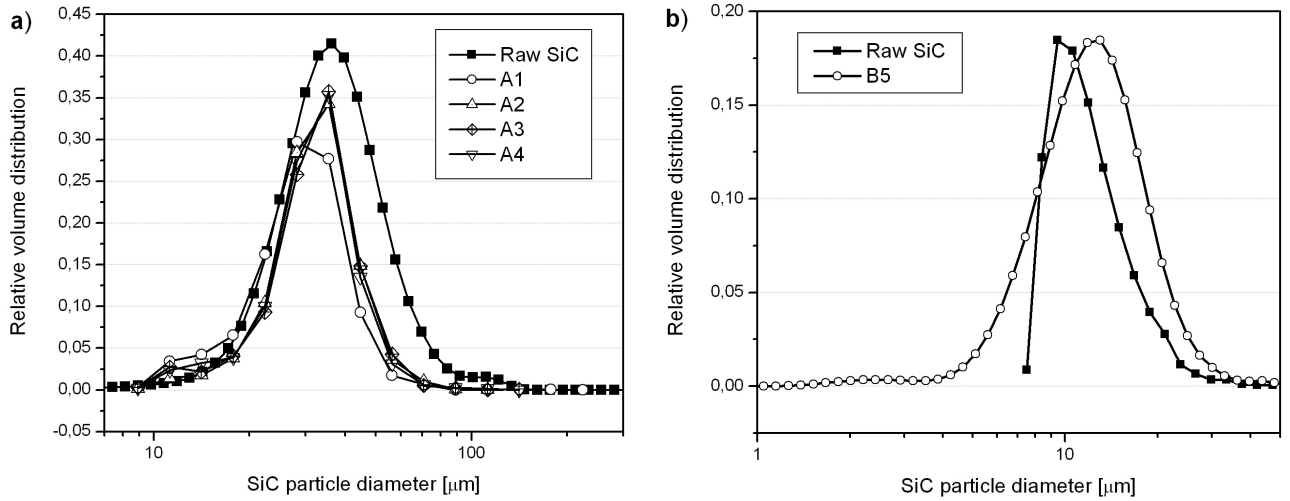


Fig. 2: Comparison between the particle size distributions measured by laser interferometry before MMC elaboration (raw SiC) and those corresponding to the reconstructed tomographic objects. **a)** 37 μm; **b)** 12 μm.

**Particle Size Effects on Particle Connectivity.** The treatment applied to the tomographic data allowed the identification of the particle clusters present in the VOIs, and the determination of the number of contacting particles in each cluster. This number is presented in the graphs in Fig. 3; there, one finds mention to "single-particle" clusters, which are no more than an expedient way to compute the number of isolated, non-contacting particles (at least up to the precision of the separation algorithm).

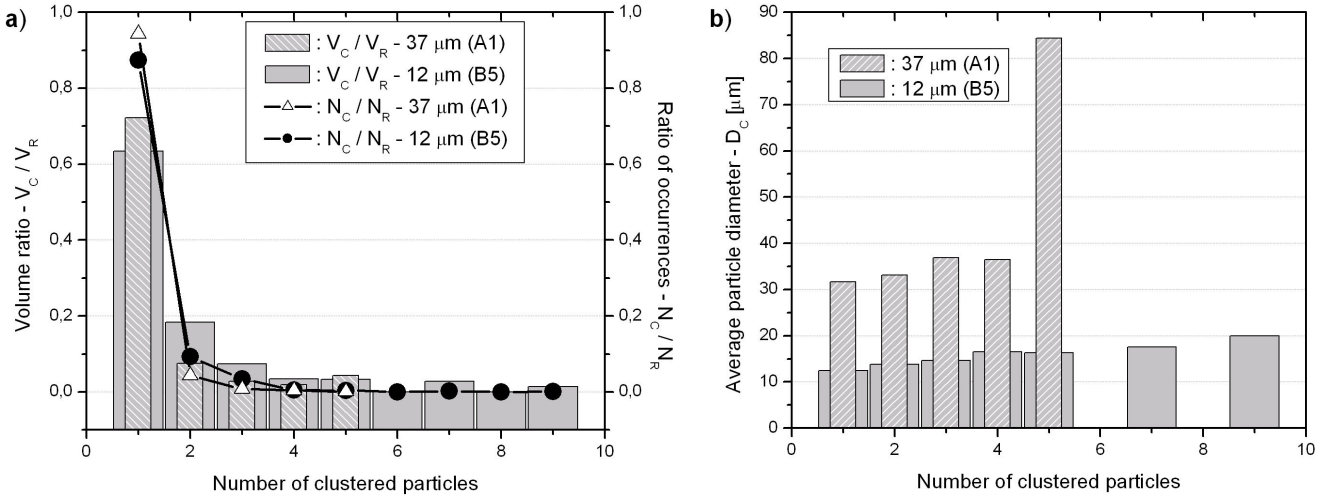


Fig. 3: Particle size effects on: **a)** volume ratio of clustered particles *vs.* overall particle volume – $V_C$ / $V_R$ – and ratio of occurrences of clustered particles *vs*. overall particle number – $N_C$ / $N_R$; **b)** average particle diameter, $D_C$.

Analysing the graph in Fig. 3a), it is seen that the smaller particles present in FGMMC B are more prone to clustering, since clusters of up to 9 particles can be found, whereas in FGMMC A no more than 5 particles can be found in any cluster. This is further confirmed by the volume ratio of particles participating in particle-particle contacts – $V_C$ – relative to the overall volume of particles – $V_R$ – since in the case of the composite reinforced by 12 μm particles, $V_C$ / $V_R$ is higher for every class of effective clusters (those not corresponding to single particles), the sole exception consisting of five-particle clusters. This behaviour is similar to what is observed by considering the number of particles, instead of its volume: the ratio $N_C$ / $N_R$ is consistently lower for the composite reinforced by 37 μm particles. It should be remarked that the number of particle contacts was not determined in

the above computations, but solely the proportions of particles with contacts, even if more than one. Also, it should be noted that as much as 94% (by number) of the 37 μm particles and 87% of those with 12 μm remain isolated in the composites; these percentages, however, decrease to 72% and 63% respectively, when particle volume is considered, indicating that within each particle population the larger particles must be more often present in the clusters than the smaller ones.

This aspect is confirmed by the graph in Fig. 3b), which represents the variation in the average contacting particle diameter – $D_C$ – among the different classes of cluster; it can be seen that the value of $D_C$ rises as more particles become present in the clusters, with a sharp increase for the case of five-particle clusters in the 37 μm –reinforced FGMMC. While the previously observed increases in the ratios $V_C / V_R$ and $N_C / N_R$ when the average reinforcement size decreases from 37 to 12 μm may be due to a higher thermodynamic difficulty to wet the smaller particles, the rise in $D_C$ within each composite when the cluster size increases must be related to a higher probability for larger particles to reach the spatial locations of others. However, at least some of the larger particle occurrences in FGMMC A could correspond to unresolved clusters of smaller particles.

**Longitudinal Variation.** Graphs similar to those previously seen are available in Fig. 4, for VOIs located along the direction of the longitudinal gradient in FGMMC A – direction $\overline{Oz}$. It can be seen, in Fig. 4a) that $N_C / N_R$ is practically independent of the position along the functional gradient; however, there is a slight increase in $V_C / V_R$ for every class of cluster when going from the surface to the interior of the material, even the volume ratio of non-contacting particles is higher in the later case. This apparent contradiction can be understood taking into account the fact that in this position no five-particle clusters were found; consequently, a fraction of the particles potentially located in that class of cluster remained available to participate in smaller clusters. As for Fig. 4-b), the observed increase in $D_C$ away from the surface is consistent with previously published results, where a dimensional gradient was observed along the longitudinal axis [3-5, 11].

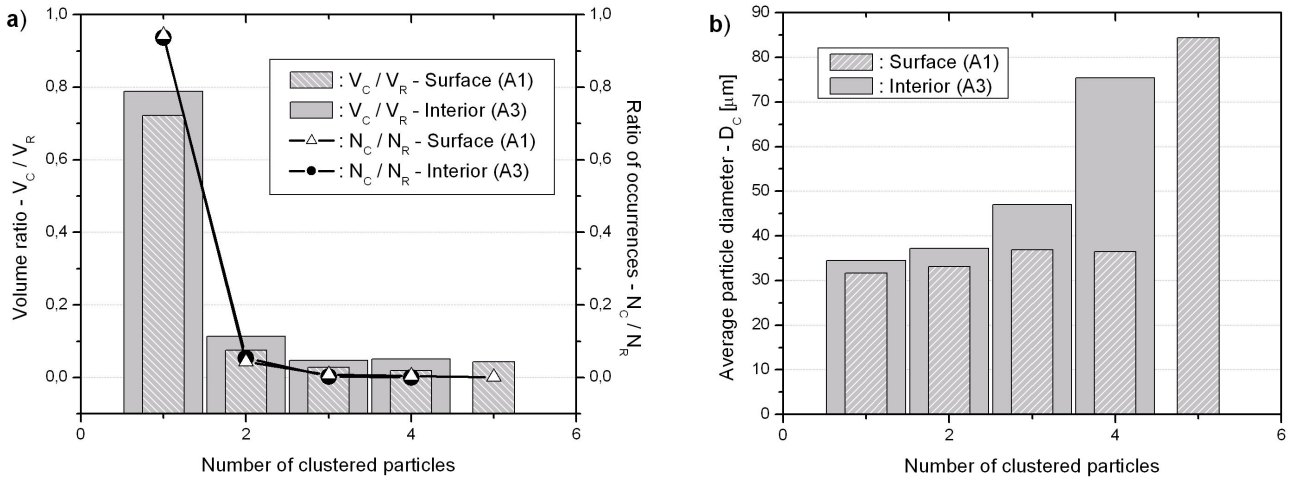


Fig. 4: Parameter variation along the direction $\overline{Oz}$ in FGMMC A: **a)** $V_C / V_R$ and $N_C / N_R$; **b)** $D_C$.

**Radial and Orthoradial Variations.** The orthoradial variation (i.e., the correlation between equivalent positions along $\overline{Ox}$ and $\overline{Oy}$) was checked, and found to be negligible for every parameter $V_C / V_R$, $N_C / N_R$ and $D_C$. Thus, in order to assess the radial variation of the same parameters along the direction $\overline{Ox}$, the statistics pertaining to VOIs A1 and A2 were combined, and compared with those from VOI A4 – Fig. 5. The most important comment is that a slightly larger fraction of particles remain unclustered close to the periphery, which can be attributed to a radial segregation effect already reported elsewhere [11].

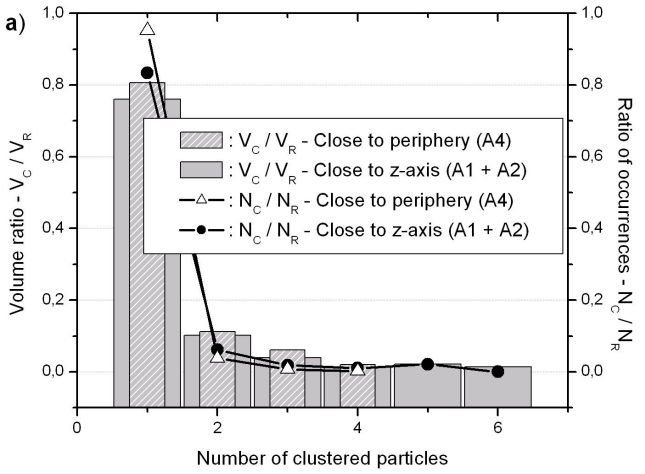


Fig. 5: Parameter variation along the direction $\overline{Ox}$, in FGMMC A **a)** $V_C$ / $V_R$ and $N_C$ / $N_R$; **b)** $D_C$.

## Conclusions

The technique of holotomography was applied to Al-$SiC_p$ FGMMC samples, in order to obtain information not accessible through conventional 2-D methods. The holographic modification of the X-ray CMT method furnished neatly contrasted images, in opposition to classical CMT. The image quality, coupled with the processing algorithm employed, led to a good agreement between the particle size evaluated by CMT and by laser interferometry. Particle clustering has been evaluated in number and volume, showing that a lower mean particle size is related to more clustering. Since molten aluminium poorly wets SiC, dispersion of smaller SiC particles is harder to achieve, thus explaining the results. Also, the mean particle size has been found to increase as a function of the number of particles within a cluster, which must be related to a higher probability for larger particles to get in contact with others. Tomographic results also supported previous observations regarding the existence of radial and dimensional segregation of the reinforcing particles in the FGMMC, as a result of the balance between the phenomena governing their distribution during centrifugal casting.

## References

[1] Y. Watanabe, N. Yamanaka, Y. Fukui: Composites Part A Vol. 29A (1998) p. 585
[2] T.W. Clyne, P.W. Withers: *An Introduction to Metal Matrix Composites* (Cambridge University Press, United Kingdom 1993) 510 pp.
[3] L.A. Rocha, A.E. Dias, D. Soares, C.M. Sá, A.C. Ferro: Ceramic Trans. Vol. 114 (2001) p. 467
[4] L. A. Rocha, P. D. Sequeira, A. Velhinho, C. M. Sá, Proc. XVI Congr. Brasileiro de Eng. Mecânica (2001) p. 381
[5] A. Velhinho, P.D. Sequeira, F. Braz Fernandes, J.D. Botas, L.A. Rocha, Mater. Sci. Forum Vol. 423-425 (2003) p. 257
[6] J.-M. Chaix: Journées d'Automne 2001 de la Société Française de Métallurgie et de Matériaux (2001) p. 80
[7] A. Velhinho, P.D. Sequeira, Rui Martins, G. Vignoles, F.M. Braz Fernandes, J.D. Botas, L.A. Rocha, Nuclear Instr. & Methods in Physics B Vol. 200 (2003) p. 295
[8] A. Velhinho, P.D. Sequeira, Rui Martins, G. Vignoles, F. Braz Fernandes, J.D. Botas, L.A. Rocha, Mater. Sci. Forum Vol. 423-425 (2003) p. 263
[9] M.I. Pech-Canul, R.N. Katz, M.M. Makhlouf, Metall. & Mater. Trans. A Vol. 31A (2000) p. 565
[10] L. Salvo, P. Cloetens, E. Maire, S. Zabler, J.J. Blandin, J.Y. Buffière, W. Ludwig, E. Boller, D. Bellet, C. Josserond, Nuclear Instr. & Methods in Physics B Vol. 200 (2003) p. 273
[11] A. Velhinho, PhD thesis, Universidade Nova de Lisboa, Portugal (2003)